Dye-enhanced multimodal confocal microscopy for noninvasive detection of skin cancers in mouse models

Jesung Park
Pawel Mroz
Michael R. Hamblin
Harvard Medical School
Massachusetts General Hospital
Wellman Center for Photomedicine
55 Fruit Street, BAR314B
Boston, Massachusetts 02114

Anna N. Yaroslavsky
Harvard Medical School
Massachusetts General Hospital
Wellman Center for Photomedicine
55 Fruit Street, BAR314B
Boston, Massachusetts 02114
    and
University of Massachusetts
Department of Physics and Applied Physics
One University Avenue
Lowell, Massachusetts 01854

Abstract. Skin cancer is the most common form of human cancer. Its early diagnosis and timely treatment is of paramount importance for dermatology and surgical oncology. In this study, we evaluate the use of reflectance and fluorescence confocal microscopy for detecting skin cancers in an *in-vivo* trial with B16F10 melanoma and SCCVII squamous cell carcinoma in mice. For the experiments, the mice are anesthetized, then the tumors are infiltrated with aqueous solution of methylene blue and imaged. Reflectance images are acquired at 658 nm. Fluorescence is excited at 658 nm and registered in the range between 690 and 710 nm. After imaging, the mice are sacrificed. The tumors are excised and processed for hematoxylin and eosin histopathology, which is compared to the optical images. The results of the study indicate that *in-vivo* reflectance images provide valuable information on vascularization of the tumor, whereas the fluorescence images mimic the structural features seen in histopathology. Simultaneous dye-enhanced reflectance and fluorescence confocal microscopy shows promise for the detection, demarcation, and noninvasive monitoring of skin cancer development. © *2010 Society of Photo-Optical Instrumentation Engineers.* [DOI: 10.1117/1.3394301]

Keywords: skin cancer; reflectance; fluorescence; confocal microscopy; contrast agents.

1 Introduction

Skin cancers, which include melanoma and nonmelanoma skin cancers (NMSC), are a major public health problem. NMSC, i.e., basal cell and squamous cell carcinomas, are disfiguring but rarely fatal. They account for more than 95% of all skin cancers, and the cost of their treatment exceeds $600 million a year. Even though melanoma is a comparatively rare form of skin malignancy, it causes more than 80% of skin cancer deaths. It is the fourth most commonly diagnosed form of cancer for men and the fifth most commonly diagnosed cancer for women in the United States. Most melanoma and NMSC are curable if diagnosed early.

Reflectance confocal microscopy is a useful adjunct to clinical histopathology. It allows for identification of malignant cells and small tumor nests *in vivo* and in real time.[1–3] However, morphology of skin in the images differs from that in histopathology. This impairs consistency of image interpretation.[4] Therefore, a well-established conventional histological stain, methylene blue (MB), has been suggested in the literature as a contrast agent to aid in confocal examination of skin cancers.[5] This practical approach enables straightforward comparison of optical images with histopathology, as skin cancers stained using MB are remarkably similar to standard Mohs *en face* frozen histopathology.[6,7] MB is United

States Food and Drug Administration (FDA) approved for *in-vivo* use and has been tested for staining various cancers *in vivo*.[8–10]

In this contribution, we investigated the use of dye-enhanced multimodal, reflectance, and fluorescence confocal microscopy for the detection of melanoma and squamous cell carcinoma in a mouse model. The goal of this study was to confirm that the *in-vivo* images of cancer stained using MB mimic the staining pattern of the hematoxylin and eosin (HE) and to demonstrate that simultaneous reflectance and fluorescence imaging provides sufficient information that can be used for effective and accurate cancer tissue discrimination.

2 Materials and Methods

2.1 Chemicals

Commercially available, pharmaceutical-grade methylene blue (MB 1% injection, USP, American Regent Laboratories,) was used. For the experiments, it was diluted to a concentration of 0.25 mg/ml with Dulbecco phosphate buffered saline solution (DPBS 1X, pH 7.4, Mediatech, Herndon, Virginia).

2.2 Cell lines

Mouse squamous cell carcinoma SCCVII and B16F10 melanoma cell lines (ATCC, Mannassas, Virginia) were cultured in RPMI medium with L-glutamine and $NaHCO_3$ supplemented with 10% heat inactivated fetal bovine serum, penicillin

Address all correspondence to: Anna N. Yaroslavsky, Harvard Medical School, Massachusetts General Hospital, Wellman Center for Photomedicine, 55 Fruit Street, BAR314B, Boston, Massachusetts 02114. Tel: 978-934-3766; Fax: 617-724-2075; E-mail: Anna_Yaroslavsky@uml.edu
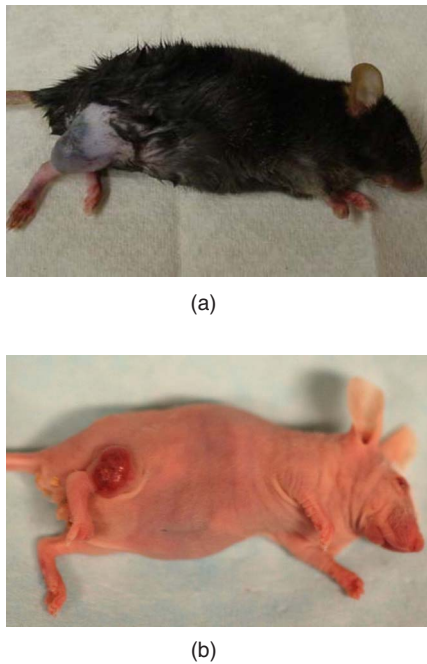
(a)

(b)

Fig. 1 Digital pictures of (a) C57/BL6 mouse with subcutaneous melanoma B16F10 and (b) BALB/c nude mouse with SCCVII.

(100 U/mL), and streptomycin (100 μg/mL) at 37 °C in 5%CO$_2$ in 75-cm^2 flasks (Falcon, Invitrogen, Carlsbad, California). All the chemicals were from Sigma in Saint Louis, Missouri.

2.3 Animal Handling

Animal experiments were approved by the Subcommittee on Research Animal Care (International Animal Care and Use Committee (IACUC)) at Massachusetts General Hospital (MGH) and were carried out in accordance with National Institutes of Health (NIH) guidelines. 6 to 8 week old male

C57BL/6 and BALB/c nude mice were purchased from Charles River Laboratories (Boston, Massachusetts) and housed in a pathogen-free environment in a MGH animal facility. C57/BL6 and BALB/c nude mice were inoculated into the thigh subcutaneously with 1000,000 cells of B16F10 and 350,000 cells of SCCVII, respectively. Two orthogonal dimensions of the tumors were measured 2 to 3 times a week with vernier calipers. 11 to 16 days after inoculation, the mice were imaged *in vivo* when the tumors reached a diameter of 10 to 14 mm. The photographs of the mice with melanoma and squamous cell carcinoma are presented in Figs. 1(a) and 1(b), respectively. Prior to imaging the mice were anesthetized using intraperitoneal injection of ketamine (90 mg/ml) and xylazine (10 mg/ml). Five minutes following anesthesia, reference reflectance and fluorescence images were acquired. Then Dulbecco's phosphate buffered saline solution (DPBS, ph 7.4) of 0.25-mg/ml MB was uniformly injected intra- and peritumorally using a 32 gauge needle. The total volume of the injection never exceeded 20 μl. 10 to 15 min after the injection, cancerous areas were imaged *in vivo*. Right after the imaging, the animals were sacrificed, and the tumors excised and immediately processed for the HE. Prior to staining, visual and microscopic examination confirmed that the blue dye was evenly distributed through the tissue.

2.4 Confocal Imaging

The schematic of the point scanning confocal microscope, used for the experiments, is presented in Fig. 2. Linearly polarized collimated light emitted by a 658-nm diode laser was used for illumination of the imaged object. The laser beam was directed onto the polarizing beamsplitter. The splitter transmitted the radiation copolarized to the incident laser light and reflected the cross-polarized light. Imaging was accomplished by point scanning the laser light in *x* and *y* directions using polygon and galvanometric mirrors, respectively. A water immersion 20×0.75 objective (Nikon, Japan) was used in all experiments. The λ/4 wave plate placed in front of the
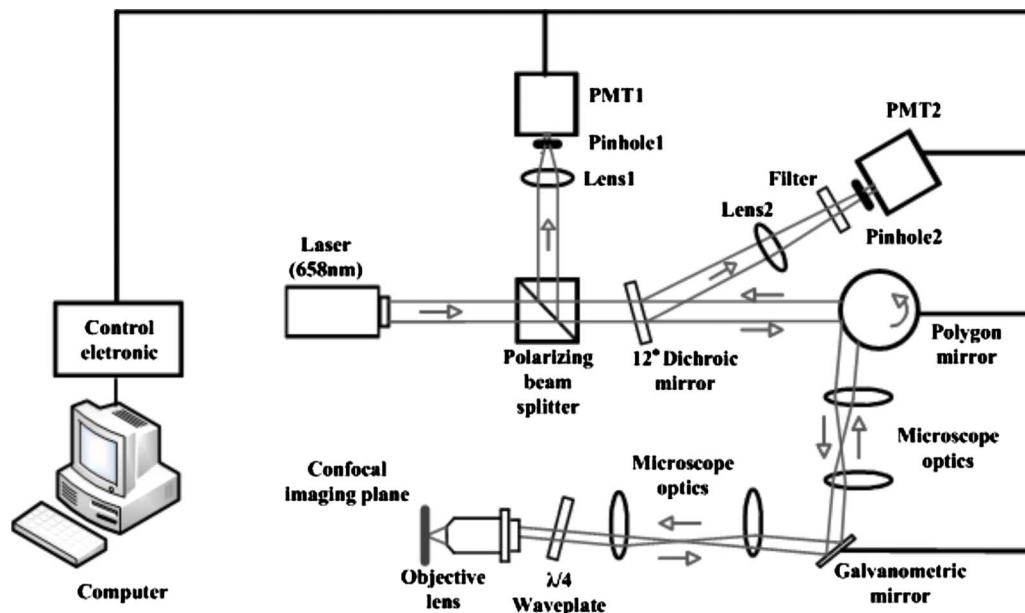

Fig. 2 Schematic of the multimodal confocal microscope.
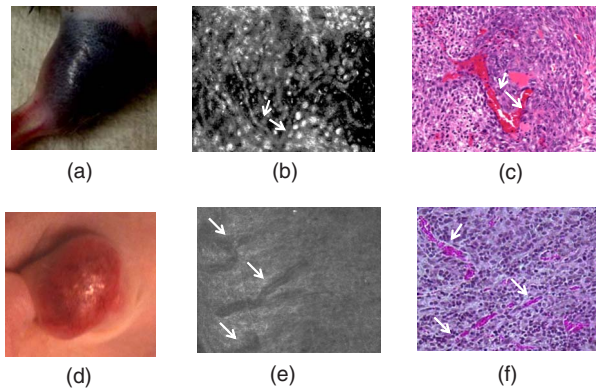
(a) (b) (c)

(d) (e) (f)

Fig. 3 Melanoma B16F10: (a) digital photograph; (b) *in-vivo* reflectance confocal image, FOV 0.8×0.6 mm. No contrast agent. (c) HE histopathology. Squamous cell carcinoma SCCVII: (d) digital photograph FOV 0.8×0.6 mm; (e) *in-vivo* confocal reflectance image, FOV 0.8×0.6 mm. No contrast agent. (f) HE histopathology, FOV 0.8×0.6 mm.

objective lens enabled registration of the light elastically remitted from the tissue using a polarizing beamsplitter. The dichroic mirror was used to transmit the elastically scattered light and reflect the fluorescence emission coming from the tissue. In addition, a narrow bandpass filter (maximal transmission at 690 nm, full width at half maximum of 20 nm) was used in the fluorescence detection channel to completely reject excitation light. The reflectance and fluorescence emissions were focused onto the pinholes and registered simultaneously by photomultiplier tubes. The system provided an axial resolution of 3.5 to 5 μm, and a lateral resolution better than 1.0 μm.

2.5 Histopathology

The mice were sacrificed immediately after imaging. Then the tumors were excised, fixed in formalin, and processed for HE histopathology. Horizontal sections were prepared from approximately the same depth and plane that was imaged. HE sections were qualitatively compared to the confocal images.

3 Results and Discussion

Examples of digital photographs, *in-vivo* reference reflectance images (i.e., images acquired before MB injection), and HE histopathology of B16F10 melanoma and SCCVII squamous cell carcinoma are presented and compared in Fig. 3. The images were acquired and the histology was processed from a depth of approximately 60 μm below the skin surface. Figure 3(a) demonstrates that due to the high melanin content of the tumor and surrounding tissue, the mouse thigh appears brown-black under white light illumination. In contrast, squamous cell carcinoma, shown in Fig. 3(d) appears red due to dense vascularization. Blood vessels are prominent and are marked with white arrows in the reference reflectance confocal images of melanoma [Fig. 3(b)] and squamous cell carcinoma [Fig. 3(e)]. Their presence and location is confirmed by corresponding HE histopathology that is presented in Figs. 3(c) and 3(f). At the same time, the appearance of melanoma and squamous cell carcinoma (SCC) cancer cells in reference confocal images differs significantly. Melanoma cells are bright because of the significant refractive index mismatch
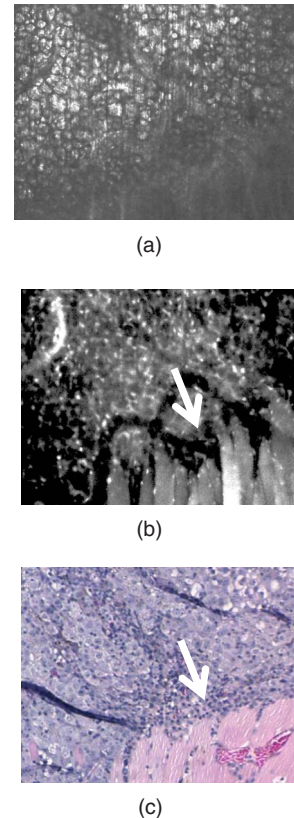

(a)

(b)

(c)

Fig. 4 *In-vivo* confocal images of a mouse thigh with melanoma B16F10. Contrast agent: 0.25-mg/ml aqueous solution of MB. FOV 0.8×0.6 mm: (a) reflectance, (b) fluorescence, and (c) corresponding HE histopathology.

with the surrounding tissue. The refractive index of melanin is ~1.7,[11] which is much higher compared to other skin constituents that exhibit refractive indices of approximately 1.37 to 1.4.[12] In contrast, SCC cells cannot be easily discerned in the reference confocal image. The refractive index of SCC is close to that of the surrounding healthy tissue, and it does not contain endogenous chromophores that absorb light in the visible spectral range. Endogenous fluorescence images of melanoma and squamous cell carcinoma lesions are not presented, as the registered signal was negligible in both cases.

Examples of the dye-enhanced *in-vivo* B16F10 melanoma images are presented side by side with corresponding HE histopathology in Fig. 4. The images were acquired from the depth of approximately 40 μm. Comparison of the optical images [Figs. 4(a) and 4(b)] to histopathology [Fig. 4(c)] confirms that melanoma cells are bright in reflectance and fluorescence *in-vivo* optical images. High content and relative refractive index of melanin explain high pixel values of melanoma cells in reflectance mode. Strong affinity of MB to the melanoma cells[13] explains the high fluorescence signal of the tumor cells in the fluorescence image. Interestingly, muscle tissue, shown with a white arrow, also accumulates a considerable amount of dye. Comparison of the fluorescence image to the corresponding HE histopathology demonstrates remarkable similarities.

Another example of the MB-stained *in-vivo* melanoma lesion images were acquired from the central area of a tumor at a depth of 70 μm. The images and histopathology are pre-
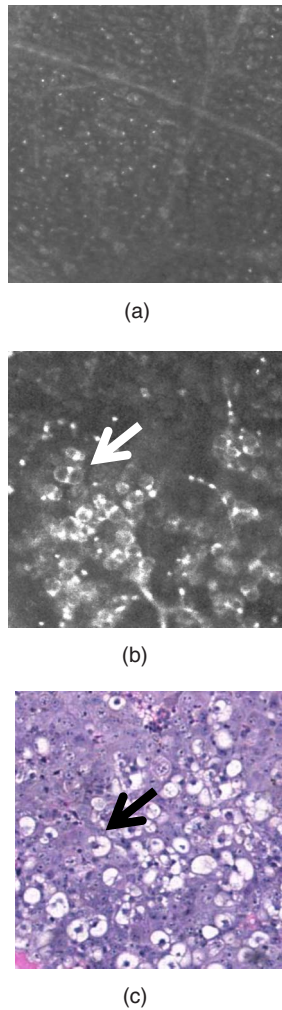
(a)

(b)

(c)

Fig. 5 *In-vivo* confocal images of a mouse thigh with melanoma B16F10. Contrast agent: 0.2-mg/ml aqueous solution of MB. FOV 0.8×0.6 mm: (a) reflectance, (b) fluorescence, and (c) corresponding HE histopathology.

(a)

(b)

(c)

Fig. 6 *In-vivo* confocal images of a mouse thigh with squamous cell carcinoma SCCVII. Contrast agent: 0.25-mg/ml aqueous solution of MB. FOV 0.8×0.6 mm: (a) reflectance, (b) fluorescence, and (c) corresponding HE histopathology.

sented in Fig. 5. The reflectance image shows highly reflective melanoma cells. Thus, the image in Fig. 5(a) does not differ much from the one shown in Fig. 4(a). However, comparison of fluorescence images to histology demonstrates that the dye is accumulated largely outside and/or on the membranes of the cancerous cells [Fig. 5(b)]. In contrast, in the fluorescence images in Fig. 4(b), the dye is located mostly inside the cells, which is consistent with the finding reported in Ref. 14 that MB binds to the mitochondria. Methylene blue molecules are positively charged, hence their high affinity to the negatively charged mitochondria. Close examination of the histopathology in Fig. 5(c) explains the differences in the localization of the dye. The cells in the center of the tumor presented in Fig. 5(c) (shown with black arrow) are undergoing autophagy due to the lack of nutrition in the central part of the lesion. Autophagy is a catabolic process that involves degradation of a cell's own components. It helps to maintain balance between the synthesis, degradation, and subsequent recycling of cellular products. It is a major mechanism by which a starving cell reallocates nutrients to the most essential processes. Histopathology shown in Fig. 5(c) (black arrow) demonstrates that
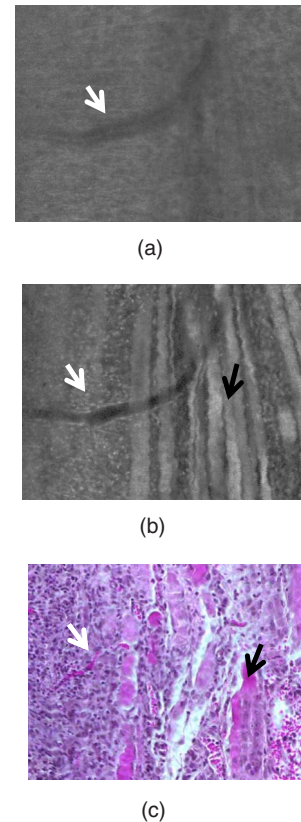
there are no organelles visible inside the cells, except for the nuclei. Thus MB does not penetrate inside the cell.

In-vivo reflectance and fluorescence images of MB-stained SCCVII squamous cell carcinoma are presented in Figs. 6(a) and 6(b), respectively. These images have been acquired from a depth of 150 μm. Corresponding HE histopathology is shown in Fig. 6(c). In the dye-enhanced reflectance image, the contrast of the cancerous cells is low. The absorption coefficient of 0.25-mg/ml aqueous solution of MB is 0.9/mm, whereas the absorption and scattering coefficients of skin are 0.1 and 9.4/mm, respectively.[15] If most of the dye accumulated in the cancerous cells, the albedo of the lesion would have decreased from 0.99 to approximately 0.9, which would have resulted in significant change in scattering. However, the contrast of reflectance images prior and after MB injection does not change. This may be due to the low dye uptake by cancer cells. At the same time, the fluorescence image in Fig. 6(b) demonstrates that this amount of dye is sufficient to provide a high fluorescence signal from cancer cells. Comparison to histopathology reveals that muscle tissue, shown with the black arrow, also takes up MB and is highly fluorescent. Analysis of the pixel values corresponding to tumor (146±48) and muscle (130±31) cells proves that the signals are comparable. This finding seemingly contradicts the accepted opinion that cancerous tissue preferentially accumulates MB. Nonetheless, our results are not surprising, as MB is not a 100% cancer-specific contrast agent. Our earlier

findings[16] indicated that due to nonspecific staining, fluorescence emission of MB can be misleading. Therefore, it is not sufficient for accurate delineation of nonmelanoma skin cancers using charge-coupled device (CCD) macroimaging. We have also proven that fluorescence polarization can be used reliably for demarcating skin cancers at low and high resolutions.[5,16] However, comparison of the image in Fig. 6(b) to histopathology, shown in Fig. 6(c) confirms that fluorescence signals mimic the structural features in the HE section at high resolution. Therefore, nonspecific MB staining is not an obstacle for image interpretation, which can be accomplished in a manner similar to histopathology.

It can be seen that an *in-vivo* reflectance image provides valuable information on vascularization, shown with a white arrow, and blood flow in the tumor. In the fluorescence image, the black trace of the blood vessel [white arrow in Fig. 6(b)] can be clearly delineated as well.

4 Summary and Conclusions

To summarize, the data presented in this contribution demonstrate the utility of multimodal confocal microscopy in combination with the selected contrast agent, i.e., methylene blue, for *in-vivo* imaging of skin cancers, including squamous cell carcinoma and melanoma, in mouse models.

We are able to acquire high quality reflectance and fluorescence images from considerable depths down to 180 μm for SCC and 70 μm for melanoma. It is worth noting that for SCC, the imaging depth was limited by the working distance of the objective lens only. For melanoma, however, the image quality deteriorated rapidly below a depth of 70 μm. These differences can be explained by the lack of endogenous chromophores and comparatively low accumulation of MB in SCCs. In melanoma, the light losses are much higher due to substantial scattering and absorption of light by melanin, combined with high MB affinity to this type of cancer cells.

Image analysis revealed that the *in-vivo* distribution of the dye is similar to that obtained in *ex-vivo* specimens.[5] Appearance of the tissue structures in fluorescence images and histopathology is remarkably similar for both types of tumor investigated. Therefore, the interpretation of *in-vivo* confocal fluorescence images in a manner similar to that of histopathology is feasible. Contrary to the accepted opinion,[8–10] we have noticed that *in-vivo* accumulation of MB in the cancerous (SCC, melanoma) and normal (muscle) tissues is comparable. Reflectance images provide important information on vascularization and blood flow of the tumor that is complimentary to the knowledge gained from fluorescence images.

Results presented in Fig. 5 demonstrate that the processes associated with cancer development, such as autophagy, can be registered *in-vivo* noninvasively by imaging exogenous fluorescence from methylene blue. MB is an FDA-approved dye, which at low volumes and concentrations is well tolerated and quickly metabolized.[17] Therefore, it can be safely used for continuous monitoring of cancer development in animals over long time periods.

Finally, we conclude that the results of this animal study support the feasibility of *in-vivo* detection of small cancer nests using multimodal reflectance and fluorescence confocal microscopy using aqueous solution of MB as a contrast-enhancing agent. The technology is capable of acquiring high quality images from depths sufficient for its use as an optical biopsy tool for NMSC in humans, and for monitoring cancer development in animals.

References

1. S. González and Z. Tannous, "Real-time, *in vivo* confocal reflectance microscopy of basal cell carcinoma," *J. Am. Acad. Dermatol.* **47**(6), 869–874 (2002).
2. S. Nori, F. Rius-Diaz, J. Cuevas, M. Goldgeier, P. Jaen, A. Torres, and S. Gonzalez, "Sensitivity and specificity of reflectance-mode confocal microscopy for *in vivo* diagnosis of basal cell carcinoma: a multicenter study," *J. Am. Acad. Dermatol.* **51**(6), 923–930 (2004).
3. A. A. Marghoob, C. Charles, K. J. Busam, M. Rajadhyaksha, G. Lee, L. Clark-Loeser, and A. C. Halpern, "*In vivo* confocal laser scanning microscopy of a series of congenital melanocytic nevi suggestive of having developed malignant melanoma," *Arch. Dermatol.* **141**(11), 1401–1412 (2005).
4. V. Q. Chung, P. J. Dwyer, K. S. Nehal, M. Rajadhyaksha, G. M. Menaker, C. Charles, and S. B. Jiang, "Use of *ex vivo* confocal scanning laser microscopy during Mohs surgery for nonmelanoma skin cancers," *Dermatol. Surg.* **30**(12), 1471–1478 (2004).
5. M. Al-Arashi, E. Salomatina, and A. N. Yaroslavsky, "Multimodal confocal microscopy for the detection of nonmelanoma skin cancers," *Lasers Surg. Med.* **39**(9), 706–715 (2007).
6. A. N. Yaroslavsky, V. Neel, and R. R. Anderson, "Demarcation of nonmelanoma skin cancer margins using multi-spectral polarized-light imaging," *J. Invest. Dermatol.* **121**(2), 259–266 (2003).
7. Z. Tannous, M. Al-Arashi, S. Shah, and A. N. Yaroslavsky, "Delineating melanoma using multimodal polarized light imaging," *Lasers Surg. Med.* **41**(1), 10–16 (2009).
8. I. J. Fedorak, T. C. Ko, D. Gordon, M. Flisak, and R. A. Prinz, "Localization of islet cell tumors of pancreas: a review of current techniques," *Surgery* **113**(3), 242–249 (1993).
9. W. B. Gill, J. L. Huffman, E. S. Lyon, D. H. Bagley, H. W. Schoenberg, and F. H. Straus, "Selective surface staining of bladder tumors by intravesical methylene blue with enhanced endoscopic identification," *Cancer* **53**(12), 2724–2727 (1984).
10. A. V. Kaisary, "Assessment of radiotherapy in invasive bladder carcinoma using *in vivo* methylene blue staining technique," *Urology* **28**(2), 100–102 (1986).
11. D. K. Sardar, M. L. Mayo, and R. D. Glickman, "Optical characterization of melanin," *J. Biomed. Opt.* **6**(4), 404–411 (2001).
12. F. A. Duck, *Physical Properties of Tissue: a Comprehensive Reference Book*, Academic Press, London (1990).
13. E. M. Link and R. N. Carpenter, "211At-methylene blue for targeted radiotherapy of human melanoma xenografts: treatment of cutaneous tumors and lymph node metastases," *Cancer Res.* **52**(16), 4385–4390 (1992).
14. A. R. Oseroff, D. Ohuoha, G. Ara, D. McAuliffe, J. Foley, and L. Cincotta, "Intramitochondrial dyes allow selective *in vitro* photolysis of carcinoma cells," *Proc. Natl. Acad. Sci. U.S.A.* **83**(24), 9729–9733 (1986).
15. E. Salomatina, B. Jiang, J. Novak, and A. N. Yaroslavsky, "Optical properties of normal and cancerous human skin in the visible and near infrared spectral range," *J. Biomed. Opt.* **11**(6), 064026 (2006).
16. A. N. Yaroslavsky, V. Neel, and R. R. Anderson, "Fluorescence polarization imaging for delineating nonmelanoma skin cancers," *Opt. Lett.* **29**, 2010–2012 (2004).
17. N. S. Magee and R. F. Wagner, "Surgical pearl: the use of methylene blue temporary tattoos for tissue orientation in Mohs micrographic surgery," *J. Am. Acad. Dermatol.* **50**(4), 640–641 (2004).